

Customization of Poly(dimethylsiloxane) Stamps by Micromachining Using a Femtosecond-Pulsed Laser**

By Daniel B. Wolfe, Jonathan B. Ashcom, Jeremy C. Hwang, Chris B. Schaffer, Eric Mazur,* and George M. Whitesides*

This work describes the use of focused, high-intensity light from a Ti:sapphire laser that generates femtosecond pulses to create topographical structure in a flat surface of poly(dimethylsiloxane) (PDMS), and the use of the PDMS surfaces patterned using this procedure for a range of purposes. PDMS patterned in surface bas-relief is the material most widely used for printing and stamping in soft lithography,^[1,2] and a material widely used in microfluidic systems.^[3] The bas-relief patterns required in these applications are usually fabricated by casting PDMS against a complementary bas-relief pattern in photoresist, fabricated in turn by photolithography. This process works well, but is not applicable to the preparation of PDMS stamps required for all types of problems; printing on spherical surfaces is an example.^[4-6]

The technique described here permits the non-photolithographic generation of surface topography for use in soft lithography and microfluidics; this technique has three useful characteristics: i) It generates features smaller than those generated by standard rapid-prototyping techniques based on printed transparency masks.^[1,2] ii) It is applicable to fabrication on non-planar surfaces. iii) It can be used in fabrication of large-area patterns. The rough, recessed features generated by this technique are useful for applications where large surface area to volume ratios are desired, e.g., in catalysis,^[7] for super-hydrophobic surfaces,^[8-10] in surface-enhanced Raman scattering,^[11,12] and as magnetic field concentrators.^[13-15] It has the disadvantages that it is a serial process, and that the laser and positioning equipment are relatively specialized. The only requirement for the material is that it must be transparent to 800 nm light: PDMS works well, but other transparent elastomeric polymers should also work.

Laser ablation is a common technique for direct writing of patterns into the surfaces of metals, semiconductors, and polymers.^[16,17] Most of the techniques that have been described for laser writing work through an absorption mechanism for light that is linear in light intensity. This sort of photochemistry typically requires doping of the material with sensitizers^[18-20] and/or the use of UV lasers.^[21,22] We have pre-

viously described the production of stamps for microcontact printing (μ CP) by ablation of a doped polymer with a diode-pumped Nd:YVO₄ laser.^[20] Line widths of the features produced through this technique are $\sim 5 \mu\text{m}$. This technique, as described, is substantially less useful than rapid prototyping. Another process, developed by Hull and co-workers, used a focused ion beam (FIB) to write patterns of sub-100 nm features into the surface of single-crystal Si $\langle 100 \rangle$.^[23] The ablated or etched features generated by both techniques were subsequently transferred into PDMS for use in soft-lithographic procedures. Johnson et al. have also demonstrated the customization of the charge of the surface of preformed microfluidic channels defined in poly(methyl methacrylate) PMMA by ablation with a UV-excimer laser.^[24] This technique modified the surface of the channel to reduce the effects of band-broadening that are characteristic of electrokinetic flow around turns. Although the resolution of both techniques is sub-micrometer, disadvantages include limited ablation range and specialized, expensive optical equipment.

Recent papers have studied the photophysics of the ablation of polymers by femtosecond lasers in detail.^[25,26] Briefly, the transfer of energy from a laser pulse with a photon energy that is less than the bandgap of the material can only occur via a nonlinear absorption mechanism. The dominant absorption process for 100 fs pulses is avalanche ionization.^[27] Avalanche ionization produces an exponential increase in conduction band electrons, but requires the presence of a small quantity of seed electrons in the conduction band; carriers thermally excited from traps or defects typically supply the necessary seed electrons. The high-intensity femtosecond pulses, even in the absence of any free carriers, can seed avalanche ionization by multiphoton ionization (MPI).^[28] Both avalanche ionization and MPI are strongly intensity-dependent. The multiphoton ionization of PDMS is at minimum a four-photon process, and thus the rate of ionization scales as I^4 (I =intensity) and sharply confines the ionization to the focal volume.

The processes of MPI and avalanche ionization increase the density of free carriers in the plasma toward the critical density, i.e., the density at which the plasma frequency is equal to that of the laser frequency. The plasma strongly absorbs the laser pulses when its density is just below the critical density; this absorption causes the kinetic energy of the free electrons to increase. Energy transfer from a 100 fs pulse to the electrons is completed before heating of the ions can occur. The end result of this process is an electron plasma with temperatures in excess of 50 000 K.^[29] Thermal equilibration between the electrons and the ions over a timescale of picoseconds drives the ions within the focal volume quickly through the melt phase to that of vaporization. Material removal, or ablation, occurs because this process imparts significant kinetic energy onto the material within the focal volume. The high temperature of the plasma decays along a steep temperature gradient that limits the spatial extent of surrounding material that is melted but not ablated.^[27] Whether used for surface ablation^[30] or bulk micromachining,^[31] the combination of a

[*] Prof. G. M. Whitesides, D. B. Wolfe
Department of Chemistry and Chemical Biology, Harvard University
12 Oxford Street, Cambridge, MA 02138 (USA)
E-mail: gwhitesides@gmwhgroup.harvard.edu

[*] Prof. E. Mazur, J. B. Ashcom, J. C. Hwang, Dr. C. B. Schaffer
Department of Physics, Harvard University
9 Oxford Street, Cambridge, MA 02138 (USA)
E-mail: mazur@deas.harvard.edu

[**] This research was supported by DARPA and used MRSEC Shared Facilities supported by the NSF under Award No. DMR-980936. D.B.W. gratefully acknowledges the NSF for a graduate fellowship. The authors thank J. Christopher Love and Abraham Stroock for helpful discussions.

low pulse energy and a steep temperature gradient leads to smaller regions of damage and less collateral damage^[27] than those observed with laser pulses of longer temporal widths.

Femtosecond pulses from a Ti:sapphire laser, when focused through a microscope objective onto the surface of PDMS, produced $\sim 1 \mu\text{m}$ features with $\sim 2 \mu\text{m}$ pitch. The depth and width of the induced damage is dependent on raster speed, pulse energy, and numerical aperture of the objective. We used the stamps produced using this procedure to fabricate microstructures by soft lithography. We also demonstrate the customization of a generic microfluidic channel to include grooves that induce transverse flows.^[32,33]

We elected to use optically flat PDMS slabs as test structures because it was relatively easy to position the surface of the slab at the focal point of the laser. The technique does not, however, require that substrates be optically flat if used in conjunction with automatic corrective positioning equipment. The principal requirement on positioning is that the surface be kept within \pm roughly one Rayleigh length of the focus ($\pm 4 \mu\text{m}$ for 0.25 NA (numerical aperture), and $\pm 1 \mu\text{m}$ at 0.45 NA, at 800 nm). The technique thus provides a route to the preparation of PDMS stamps on topologically complex surfaces.^[4-6,34,35] Figure 1 describes the process for preparation of the PDMS slabs. The glass slide on the back provides support for the flexible PDMS slab while mounted in the path of the laser beam. We found 1 mm thick samples of PDMS to be sufficiently mechanically stable to be manipulated for soft lithography.

PDMS stamps having bas-relief structures generated by ablation with both 0.25 and 0.45 NA objectives are shown in Figure 2. The resolution limit of the technique depends on the

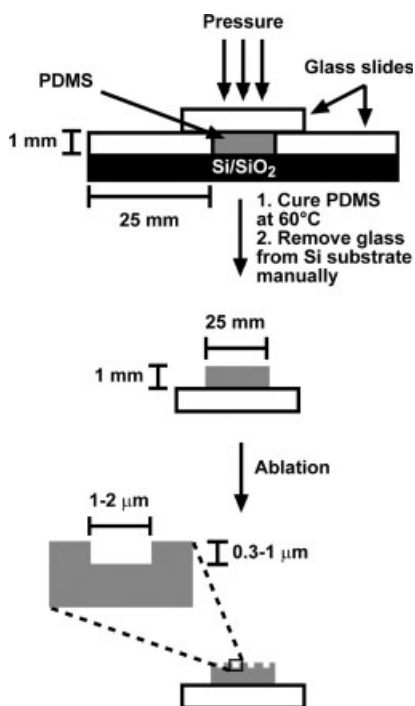


Fig. 1. Schematic diagram of the preparation of optically flat PDMS and the subsequent laser writing.

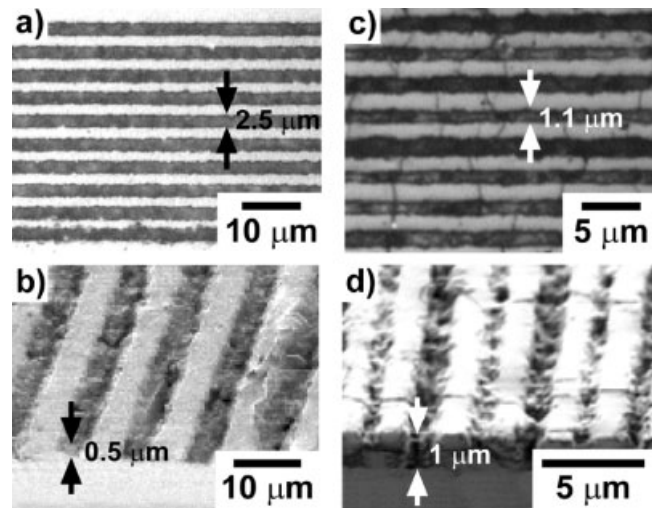


Fig. 2. Laser writing of lines on slabs of PDMS with two different objectives. a) Optical micrograph of lines written with a 0.25 NA objective. The pulse energy was 80 nJ and the scan speed was $100 \mu\text{m s}^{-1}$. The widths of these features were intentionally chosen to demonstrate the limits of resolution of this technique. b) SEM micrograph of the cross-section of the lines in (a). c) Optical micrograph of lines written with a 0.45 NA objective. The pulse energy was 40 nJ and the scan speed was $200 \mu\text{m s}^{-1}$. d) SEM micrograph of the cross-section of the lines in (c). The PDMS stamps in each image were sputter coated with a thin layer of Au to reduce charging of the surface. The cracks in images (b) and (d) are the result of stress-induced cracking of a layer of gold deposited on the PDMS stamp.

size of the focused spot, and on the mechanism of non-linear absorption. At 0.25 NA, structures are limited to widths of $\sim 2 \mu\text{m}$ spaced by a minimum distance of $\sim 2.5 \mu\text{m}$ (Figs. 2a,b). The larger focal volume at 0.25 NA causes collateral damage and ablation to neighboring lines when we attempted to write patterns with smaller pitch. Increasing the NA to 0.45 permits the writing of $\sim 1 \mu\text{m}$ lines spaced by $\sim 2 \mu\text{m}$ (Figs. 2c,d). Again we were limited in pitch due to collateral damage to neighboring structures. The depth of the trenches is between 0.3 and $1 \mu\text{m}$; this depth is relatively independent of the NA used, but correlates with raster speed and focal volume of the spot on the surface. Even with constant raster speed, however, we observe variations in trench depth. We attribute this variation to the difficulty of positioning the beam such that the focal volume at the surface is constant during every run. Although the bottom of the ablated areas is uneven, their texture is not relevant to the use of these features for μCP .

A cover slip must be in place between the objective and the sample to prevent ablated material from coating the optics of the objective. Objectives used have $\text{NA} < 0.5$ because ablation requires a small gap between the cover slip on the objective and the surface of the PDMS slab. High NA objectives have working distances that are too small to allow for sufficient space between the PDMS and the objective. The short confocal parameter of the higher NA objectives also makes it difficult to keep the beam focused on the surface.

We wrote a test pattern consisting of crosses in a square array on the surface of PDMS using this technique. Figure 3 shows the results of stamp preparation and use of the stamp in μCP , solvent-assisted micromolding (SAMIM), and micro-

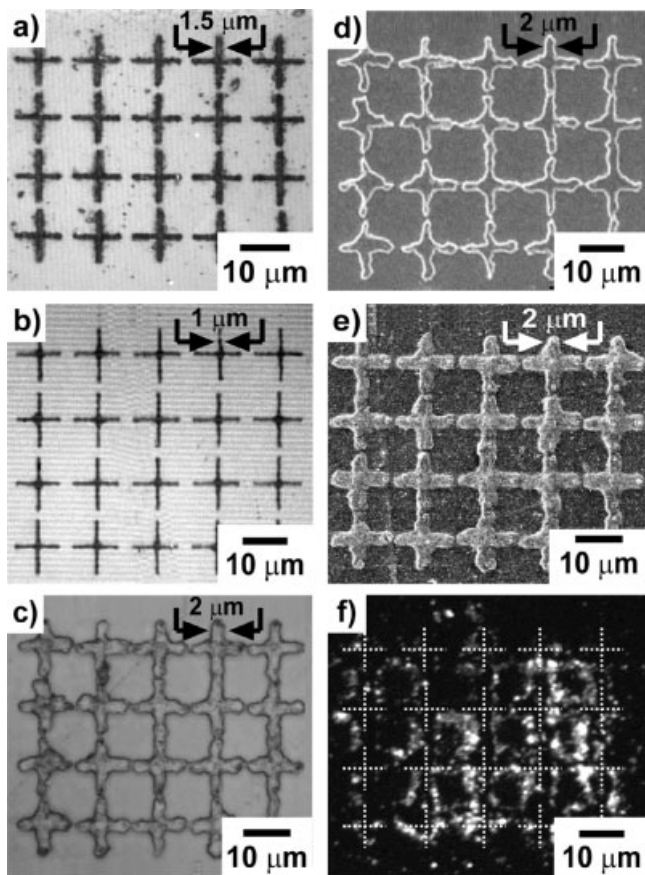


Fig. 3. a) Optical micrograph of a PDMS stamp prepared by the technique. A 0.45 NA objective was used with pulse energy of 30 nJ and scan speed of $100 \mu\text{m s}^{-1}$. b) SEM micrograph of a sample prepared by μCP with the stamp in (a). The light regions are gold and the dark regions are the silicon substrate. c) Optical micrograph of a sample prepared by SAMIM. d) SEM micrograph of the sample from (c) after the reactive ion etching of the unprotected silicon. The photoresist has been removed to reveal the features made of Si. e) SEM micrograph of magnetic field concentrators made of *mPDMS*. f) Fluorescence optical micrograph of the field concentrators after exposure to fluorescently-labeled, paramagnetic particles. The white, dotted crosses indicate the location of the field concentrators.

transfer molding (μTM). The line widths of the μCP pattern are about a factor of two smaller than those of the stamp. We attribute this decrease in line width to the curved profile of the trenches written in the PDMS. This profile allows the contact area of the stamps to be larger than that expected from the scanning electron microscopy (SEM) images. This phenomenon has been documented in previous work^[36] and can be used to our advantage to prepare features with line widths of $< 1 \mu\text{m}$.

The roughness of the ablated PDMS mold limits its use as a template for the fabrication of features by molding. Surface morphology does not affect the ability of the molded structures to act as an etch-resistant mask for reactive ion etching (RIE). We prepared features made of photoresist on a Si/SiO₂ wafer by SAMIM (Fig. 3c).^[37] Reactive ion etching with CF₄ etches the silicon $\langle 100 \rangle$ substrate preferentially over the resist. The subsequent removal of the photoresist with acetone reveals the features transferred into the silicon (Fig. 3d).

To demonstrate an application of the features replicated from these stamps, we prepared magnetic field concentrators by μTM of nickel-doped, magnetic PDMS (*mPDMS*).^[38] Figures 3e and f are images of the field concentrators before and after introduction of fluorescently-labeled paramagnetic beads. The features concentrate the magnetic field of a permanent magnet placed below the substrate. The magnetic beads are trapped at the high-field-gradient sites localized around the features. The untrapped beads are washed away with water.

The technique is also useful for customizing structures defined in PDMS that are prepared from a common master. The addition of grooves to a generic microfluidic channel is one example of a useful modification of a PDMS-based device. We and others have previously demonstrated that grooves aligned at an oblique angle with respect to the long axis of the microfluidic channel can induce transverse flows at low Reynolds numbers.^[32,33] Transverse flows are useful for mixing two or more liquids as they flow axially through a microfluidic channel.

The generic microfluidic channel was prepared as described previously.^[3] We used the technique to write grooves in the PDMS channel with approximately the same depth, width, and pitch as the height of the microfluidic channel ($\sim 10 \mu\text{m}$). Figure 4a is a schematic diagram of the three-dimensional twisting flow of fluids caused by the pat-

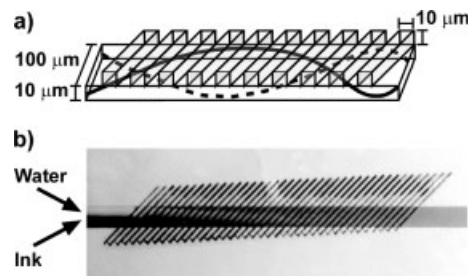


Fig. 4. a) Schematic diagram of the twisting flow of two liquids (solid and dashed lines) in a microfluidic channel patterned with grooves on one face. The dimensions shown are those of the channel in (b). b) Optical micrograph of two streams of liquids (water (light) and ink (dark)) as they flow axially through the channel. The dark lines, oriented 45° to the long axis of the channel, are grooves in the top of the channel. The grooves extend beyond the length of the channel and these regions are filled with stagnant fluid.

terned grooves. Figure 4b shows the laminar flow of water and an aqueous ink solution^[39] through the channel under a pressure gradient generated by applying a weak vacuum to the outlet of the channel. The fluids mix quickly once the transverse motions of the fluids begin, and are completely mixed as they exit the region with grooves. This simple transverse flow increases the rate of mixing significantly because of the low aspect ratio of the channel (10:1 width to height). The transverse rotation of the two streams reduces the distance in the channel over which diffusion completely mixes the two streams from $100 \mu\text{m}$ (i.e., across the channel) to $10 \mu\text{m}$ (i.e., from top to bottom of the channel). The time required to mix the streams accordingly decreases by a

factor of 100 ($\Delta t \sim \Delta x^2/D$, where t = time, x = distance, and D = diffusivity).

This paper demonstrates the use of a pulsed, femtosecond Ti:sapphire laser to write patterns in PDMS stamps for use in soft lithography and to customize a microfluidic channel defined in PDMS. This process is a non-photolithographic technique to prepare PDMS stamps with features as small as 1 μm in width and 2 μm in pitch over large areas ($> 20 \text{ mm}^2$) rapidly ($\sim 15 \text{ min}$).^[40] An advantage of the technique over molding is that the features are fabricated in PDMS that has already been cured; the features are therefore not subject to any dimensional changes resulting from curing of the PDMS. This technique may be most useful for the customization of PDMS structures that are fabricated from a common template. Such an application extends the capabilities of soft-lithographic techniques to the rapid prototyping of devices that derive their characteristic properties from small modifications in the overall structure.

Experimental

A silicon wafer was exposed to tridecafluoro(1,1,2,2-tetrahydrooctyl)-1-trichlorosilane ($\text{CF}_3(\text{CF}_2)_5\text{CH}_2\text{CH}_2\text{SiCl}_3$) (United Chemical Technologies, Bristol, PA) in vacuum for 1 h to lower the surface free energy of the wafer; this coating allows removal of the PDMS slab from the silicon substrate. PDMS slabs were prepared by curing PDMS prepolymer at 60 °C for 3 h while it was sandwiched between a glass slide and a silicon wafer under pressure. The PDMS slab was removed from the silicon wafer while still attached to the glass slide.

Laser ablation: The laser chain was a home-built, regeneratively-amplified, Ti:sapphire laser operating at 800 nm and producing 100 fs pulses at 1 kHz. To ensure diffraction-limited focusing, the beam was expanded to three times the diameter of the back aperture of the objective; it produced nearly flat-field illumination. A cover slip was attached to the front of the objective to prevent ablated material from collecting on the lens. The PDMS slab was mounted on a computer-controlled, three-axis, translation stage, and aligned such that the surface stays in the focus upon translation in the plane of the surface. Typical translation speeds were between 50 $\mu\text{m s}^{-1}$ and 200 $\mu\text{m s}^{-1}$. The speed of translation across the surface was inversely proportional to the width of the features obtained due to the change in the time of exposure of the PDMS by the laser in one spot. Features written at high speeds were rough as a result of the vibration of the stage itself.

Microcontact Printing: Microcontact printing was carried out as described previously [1,2]. Briefly, a 10 mM solution of octadecanethiol in ethanol was wiped across the surface of the stamp with a cotton swab and the ethanol was allowed to evaporate in a stream of N_2 for 1 min. The stamp was placed manually against a gold-coated (30 nm Au/5 nm Cr) Si/SiO₂ wafer and removed within 5 s of wetting the surface. The unprotected gold was etched using a ferri/ferrocyanide based etch composed of $\text{K}_2\text{S}_2\text{O}_8$ (0.1 M), $\text{K}_3\text{Fe}(\text{CN})_6$ (0.01 M), $\text{K}_4\text{Fe}(\text{CN})_6$ (0.001 M), and KOH (0.1 M) [41].

Solvent-Assisted Micromolding: [37] The PDMS stamp was oxidized for 20 s at 2 torr in an oxygen plasma (generated in a plasma cleaner; Harrick PDC-23G) and exposed to (tridecafluoro-1,1,2,2-tetrahydrooctyl)-1-trichlorosilane in vacuum for 1 h. A layer of photoresist (Shipley 1805, Chelmsford, MA) was spun onto the wafer at 5000 rpm. The stamp was coated with a small amount of isopropyl alcohol and then was placed immediately in contact with the photoresist. The solvent was allowed to evaporate over 15 min and the stamp was removed manually to reveal the features.

Microtransfer Molding: The stamp was prepared in the same manner as above prior to molding. The magnetic PDMS (*m*PDMS) was prepared by mixing the standard components of PDMS with nickel powder (50 wt.-%, Alfa Aesar, 0.08–0.15 μm). A small drop of the mixture was placed onto the stamp and a small piece of PDMS was used as a scraper/wiper to remove excess *m*PDMS. The *m*PDMS-filled mold was sandwiched between a silicon wafer and glass slide and clamped into place. The *m*PDMS was cured for 3 h at 60 °C. The PDMS mold was removed by wetting with EtOH to help preserve small structures.

Received: September 2, 2002
Final version: October 8, 2002

- [1] Y. Xia, G. M. Whitesides, *Angew. Chem. Int. Ed.* **1998**, *37*, 550.
- [2] Y. Xia, G. M. Whitesides, *Annu. Rev. Mater. Sci.* **1998**, *28*, 153.
- [3] J. C. McDonald, G. M. Whitesides, *Acc. Chem. Res.* **2002**, *35*, 491.
- [4] R. Jackman, J. Wilbur, G. M. Whitesides, *Science* **1995**, *269*, 664.
- [5] R. J. Jackman, S. T. Brittain, A. Adams, M. G. Prentiss, G. M. Whitesides, *Science* **1998**, *280*, 2089.
- [6] R. J. Jackman, S. T. Brittain, A. Adams, H. Wu, M. G. Prentiss, S. Whitesides, G. M. Whitesides, *Langmuir* **1999**, *15*, 826.
- [7] G. A. Somorjai, *J. Phys. Chem. B* **2002**, *106*, 9201.
- [8] M. Miwa, A. Nakajima, A. Fujishima, K. Hashimoto, T. Watanabe, *Langmuir* **2000**, *16*, 5754.
- [9] S. Lazare, V. Granier, P. Lutgen, G. Feyder, *Rev. Phys. Appl.* **1988**, *23*, 1065.
- [10] M. Thieme, R. Frenzel, S. Schmidt, F. Simon, A. Henning, H. Worch, K. Lunkwitz, D. Scharnweber, *Adv. Eng. Mater.* **2001**, *3*, 691.
- [11] J. A. Sanchez-Gil, J. V. Garcia-Ramos, E. R. Mendez, *Lec. Notes Phys.* **2000**, *534*, 215.
- [12] I. H. Lee, S. W. Han, K. Kwan, *J. Raman Spectrosc.* **2001**, *32*, 947.
- [13] B. L. Hirschbein, D. W. Brown, G. M. Whitesides, *CHEMTECH* **1982**, *12*, 172.
- [14] R. Gerber, R. Birss, *High Gradient Magnetic Separation*, Research Studies, New York **1983**.
- [15] J. Svoboda, *Magnetic Methods for the Treatment of Minerals*, Elsevier, Amsterdam, The Netherlands **1987**.
- [16] J. J. Dubowski, M. Julier, G. I. Sproule, B. Mason, *Mater. Res. Soc. Symp. Proc.* **1996**, *397*, 509.
- [17] A. Yabe, *Springer Ser. Mater. Sci.* **1999**, *35*, 171.
- [18] T. Lippert, T. Kunz, C. Hahn, A. Wokaun, *Recent Res. Dev. Macromol. Res.* **1997**, *2*, 121.
- [19] A. Athanassiou, M. Lassithiotaki, D. Anglos, S. Georgiou, C. Fotakis, *Appl. Surf. Sci.* **2000**, *154*, 89.
- [20] B. A. Grzybowski, R. Haag, N. Bowden, G. M. Whitesides, *Anal. Chem.* **1998**, *70*, 4645.
- [21] E. A. Waddell, L. E. Locascio, G. W. Kramer, *JALA* **2002**, *7*, 78.
- [22] A. Costela, *Rev. Plast. Mod.* **1994**, *68*, 438.
- [23] D. M. Longo, W. E. Benson, T. Chraska, R. Hull, *Appl. Phys. Lett.* **2001**, *78*, 981.
- [24] T. J. Johnson, D. Ross, M. Gaitan, L. E. Locascio, *Anal. Chem.* **2001**, *73*, 3656.
- [25] H. Kumagai, K. Midorikawa, K. Toyoda, S. Nakamura, T. Okamoto, M. Obara, *Appl. Phys. Lett.* **1994**, *65*, 1850.
- [26] S. Baudach, J. Bonse, W. Kautek, *Appl. Phys. A: Mater. Sci. Process.* **1999**, *69*, S395.
- [27] X. Liu, D. Du, G. Mourou, *IEEE J. Quantum Electron.* **1997**, *33*, 1706.
- [28] M. Lenzner, J. Kruger, S. Sartania, Z. Cheng, C. Spielmann, G. Mourou, W. Kautek, F. Krausz, *Phys. Rev. Lett.* **1998**, *80*, 4076.
- [29] B. C. Stuart, M. D. Feit, S. Herman, A. M. Rubenchik, B. W. Shore, M. D. Perry, *Phys. Rev. B* **1996**, *53*, 1749.
- [30] D. von der Linde, K. Sokolowski-Tinten, J. Bialkowski, *Appl. Surf. Sci.* **1997**, *109–110*, 1.
- [31] C. B. Schaffer, A. Brodeur, J. F. Garcia, E. Mazur, *Opt. Lett.* **2001**, *26*, 93.
- [32] A. Ajdari, *Phys. Rev. E* **2002**, *65*, 016301.
- [33] A. D. Stroock, S. K. W. Dertinger, A. Ajdari, I. Mezic, H. A. Stone, G. M. Whitesides, *Science* **2002**, *295*, 647.
- [34] H. Wu, S. T. Brittain, J. R. Anderson, B. Grzybowski, S. Whitesides, G. M. Whitesides, *J. Am. Chem. Soc.* **2001**, *122*, 12 691.
- [35] Y. Xia, E. Kim, X.-M. Zhao, J. A. Rogers, M. Prentiss, G. M. Whitesides, *Science* **1996**, *273*, 347.
- [36] E. Delamar, H. Schmid, A. Bietsch, N. B. Larsen, H. Rothuizen, B. Michel, H. Biebuyck, *J. Phys. Chem. B* **1998**, *102*, 3324.
- [37] E. Kim, Y. Xia, X.-M. Zhao, G. M. Whitesides, *Adv. Mater.* **1997**, *9*, 651.
- [38] S. Palacin, P. C. Hidber, J.-P. Bourgin, C. Miramond, C. Fermon, G. M. Whitesides, *Chem. Mater.* **1996**, *8*, 1316.
- [39] We diluted the water and ink solutions with ethanol (10:1) to limit the formation of bubbles.
- [40] Commercially available Ti:sapphire lasers have repetition rates of $> 100 \text{ kHz}$. This increase in the repetition rate decreases the time necessary for ablation by a factor of ~ 100 , and permits an increase in the translation speed from 200 $\mu\text{m s}^{-1}$ to 10 mm s^{-1} (this speed is near the maximum available for reasonable-cost motorized translation stages). The combination of the increased repetition rate and the increased translation speed reduces the overall time to write a 20 mm^2 stamp with lines of 1 μm and a pitch of 2 μm from $\sim 14 \text{ h}$ to $\sim 900 \text{ sec}$, or $\sim 15 \text{ min}$.
- [41] Y. Xia, X.-M. Zhao, E. Kim, G. M. Whitesides, *Chem. Mater.* **1995**, *7*, 2332.